Pak. J. Bot., 58(8) August 2026.

ARTICLE DOI: http://dx.doi.org/10.30848/PJB2026-8(16)

POTENTIAL OF Se AND Se/CuO NANOPARTICLES FOR ENHANCING GROWTH AND BIOCHEMICAL TRAITS OF CLOVER PLANTS UNDER THE COMBINATION OF SALINITY AND Pb STRESS WITH REFERENCE TO ITS ANTIMICROBIAL AND ANTIOXIDANT PROPERTIES

ABEER S. MEGANID[1] AND ABDELATTI I. NOWWAR[2]

[1]College of Science and Humanities, Jubail, Imam Abdulrahman Bin Faisal University, Jubail, Saudi Arabia
[2]Botany and Microbiology Department, Faculty of Science, Al-Azhar University, Cairo, Egypt

*Corresponding author's email: abdelatti.ibrahim@azhar.edu.eg

Abstract

In the development of sustainable agriculture, nanotechnology has shown promise in resolving abiotic issues, especially those pertaining to salt stress and heavy metal tolerance. To validate the spherical morphology and crystalline framework of the synthesized nanomaterials, investigators deployed X-ray diffraction (XRD), Fourier transform infrared spectroscopy (FTIR), and transmission electron microscopy (TEM). Subsequent dimensional analysis via ImageJ software revealed mean diameters of 34.1 nm for the selenium/copper oxide nanoparticles (Se/CuO NPs) and 33.8 nm for the isolated selenium nanoparticles (Se NPs). The production of these particles relied on a highly cost-effective and accessible green synthesis protocol, specifically utilizing an extract derived from *Mentha viridis* L. (mint leaves). The selenium/copper oxide nanoparticles demonstrated strong antibacterial and antioxidant qualities as well as plant growth-promoting effects when exposed to salt and heavy metals at the same time. Alfalfa plants' morphological characteristics and biochemical markers (pigments, proteins, carbohydrates, proline, and antioxidant enzymes), which normally decline under stressful circumstances, were enhanced by the addition of selenium/copper oxide nanoparticles. In comparison to Se nanoparticles, the Se/CuO nanoparticles demonstrated greater inhibition zones against *Enterococcus faecalis* bacteria, up to 40 mm, according to antimicrobial testing. Remarkably, lead levels were lowered by 25.12% when Se/CuO nanoparticles were present at a concentration of 50 ppm. Additionally, they showed greater antioxidant capacity than Se nanoparticles. These findings highlight the viability of employing bioengineered bimetallic nanoparticles to improve clover plant resilience and reduce stress.

Key words: *Mentha viridis*; Nanoparticles; Heavy metals; Stress; Antimicrobial

List of abbreviation: NPs; Nanoparticles, DPPH; 1,1-diphenyl-2-picrylhydrazyl, Cat; Catalase, POX; peroxidase, PPO; poly phenol oxidase, HMs; Heavy metals, Pb; Lead, ROS; Reactive oxygen species

Introduction

Climate change-related abiotic stressors impede plant growth and productivity; Salinity and heavy metal toxicity are two significant abiotic stressors that lower crop yields globally and affect food security (Khalid *et al.,* 2022). In our study, we assessed the morphological and biochemical changes in Clover plants under the combined stresses of salinity and heavy metal exposure. Heavy metals are non-degradable contaminants in soil matrices that have high environmental mobility and toxicity, posing serious threats to ecosystems and human health. Special emphasis is needed on elements such as chromium, cadmium, nickel, mercury, and lead because they are particularly toxic and disrupt important agronomic functions in plant systems. These metals are very reactive because they exist in high oxidation states; therefore, they disrupt all aspects of plant functioning from a cellular to molecular standpoint. This disruption of biochemistry in plants inhibits photosynthesis and changes enzymatic functions in plant tissue (Yaashikaa *et al.,* 2022). Therefore, it is expected that there will be a significant decrease in agricultural production worldwide as the world's population is predicted to grow to approximately 8.54 billion by 2030 (a 70% increase in the world's population); therefore, there needs to be a significant increase in agricultural production. Thus, methods need to be developed to remove or stabilize heavy metals in contaminated agricultural soils (Sampantamit *et al.,* 2021). Also, salinity negatively impacts the stages of germination and seedling development. Particular ion toxicity, nutritional imbalance, and a reduction in the osmotic potential of growing media are all associated with salt's negative impacts on plant growth (Atta *et al.,* 2023).

Among various methodologies explored to bolster plant resilience and alleviate the severe impacts of abiotic stress, nanoparticle utilization stands out as a highly viable approach. Research indicates these agents effectively promote vegetative development amidst adverse environmental constraints (Khaled *et al.,* 2022). As a result, the present study used biocompatible selenium nanoparticles together with bimetallic selenium/copper oxide nanoparticles. The main aim was to counteract the joint,

Received: 25-11-2025 | Revised: 19-02-2026 | Accepted: 25-02-2026 | Online: 14-04-2026

adverse impact of the heavy metal toxicity and salinity on botanical systems. Such particles can be considered as the potential ones to mitigate stressful situations in agro-environmental conditions due to the high volume-to-surface ratio that provides a high chemical reactivity and allows changing physical characteristics of the substrate (Das & Das, 2019). Research has shown that nanoparticles are one of the best methods to enhance plant growth and increase its lifespan in saline stress (Das & Das, 2019).

Organic matrices have been used to synthesize bimetallic NPs using single or dual components that have the potential to be applied in pharmaceutical and biomedical fields (Al-Rajhi *et al.,* 2024). Another environmentally friendly and sustainable approach to NP synthesis is the use of biological methods in place of traditional synthetic procedures to prepare NPs (Abdelghany, 2013; Qanash *et al.,* 2024). Plant-derived extracts provide an efficient platform with which nanoparticle (NP) can be synthesized as opposed to microbial methods. Such efficiency is due to a highly diverse array of biomolecules, i.e. phenolic acids, alkaloids, and phenolics, which act as native oxidizing and reducing agents and quickly convert metallic ions into stable colloidal nanoparticle dispersions (Soliman *et al.,* 2024; Amin *et al.,* 2024, 2025). Moreover, Selenium nanoparticles (Se NPs) have also been of great interest because of their new formulations with other types of metal nanoparticles and their wide range of application in biomedical, agricultural, and nutrition applications (Safdar *et al.,* 2023). Recently, Elkady *et al.,* (2025) emphasized the anticancer, antiviral, and antibacterial activity of CuO/Se NPs using an eco-friendly green synthesis method and showed a significant potential even at non-toxic levels. There is limited experimental evidence on nanoparticles (NPs) effects in plant systems that are exposed to two environmental stressors, namely salinity and heavy metals (HMs).

This paper introduces new selenium nanoparticles (Se NPs) and selenium/copper oxide nanoparticles (Se/CuO NPs) of Mentha viridis leaf extract the first botanical source to be utilized. The researchers tested the hypothesis on whether these nanoparticles decrease the negative physiological responses in clover samples which were treated with lead (Pb) and salt at the same time. The antibacterial and antioxidant properties of the nanoparticles generated were fully evaluated. The experimental set up was constructed through the plant tolerance mechanisms in the coupled abiotic stress conditions. The biological activity of the two nanoparticle compositions was also explored other than their role in alleviating stress.

Materials and Methods

Preparation of *Mentha viridis* leaf **extract:** *Mentha viridis* L. specimens were obtained by the researchers in the botanical garden of the Faculty of Science, Department of Botany, Al-Azhar University. The biomass collected was washed with deionized distilled water by the team, and then allowed to undergo a period of five days of desiccation at ambient temperatures in a shaded place. Then, the final 100 ml volume of 5 g of the resulting pulverized leaves was heated to 70^{o}C in deionized double-distilled water. Lastly, this hot mixture was elucidated under Whatman No. 1 filter paper at 4^{o}C.

Synthesis of Se NPs and Se/CuO NPs: In order to start the synthesis of selenium nanoparticle (Se NPs), the researchers initially modified the pH of the reaction to 7.4 by using 0.1 M potassium hydroxide. Following this stabilization step, 30 mL of aqueous peppermint extract was continuously stirred into an equal volume of 0.02 mM sodium selenite. Ultra sonification was performed for 1 h, yielding red selenium nanoparticles Vahdati & Moghadam (2020). In order to create bimetallic selenium/copper oxide nanoparticles, equal amounts of sodium selenite solution (0.02 mM) and copper sulfate solution (0.01 mM) were combined to create a 60 mL mixture, which was subsequently heated to 80 °C for ten minutes. After adding 30 mL of a plant extract, the mixture was put in an Eppendorf tube and magnetically agitated for one hour at 40°C. The fact that there was observable change in color of the product to a greenish-black color was an affirmation that the production of the selenium/copper oxide nanoparticles was successful. Centrifugation at 10,000 rpm was used to collect such nanomaterials. To eliminate the rest of the impurities, the group washed the collected pellet using the double-distilled deionized water a number of times. Finally, the samples were dried in an 80^{o}C oven followed by preserving them in 4 ^{o}C until they were required to be utilized in the subsequent experiments.

Characterization of the biogenic nanoparticles: Various spectroscopic techniques were used in order to characterize the nanoparticles (NPs). The nature of the constituent composition and crystalline structure were verified in energy-dispersive X-ray spectroscopy (EDX). The high-resolution transmission electron microscopy (HR-TEM) simplified the determination of the size and morphological characteristics of the particles. It was through the Fourier transform infrared spectroscopy (FTIR) that the functional groups that were involved in the stabilizing activity of the nanoparticles could be identified.

Assessment of the impact of selenium nanoparticles and bimetallic selenium/copper oxide nanoparticles on the growth of clover plants under stress conditions: Researchers procured Egyptian clover (*Trifolium alexandrinum*) germplasm from Egypt's Giza Agricultural Research Center. Subsequently, the team executed a controlled pot trial utilizing a sandy loam substrate within the Faculty of Science's botanical garden at Al-Azhar University. In the experiment, 10 treatment groups of clover plants were used as illustrated in Table 1. These groups were control group (water sprinkled), stressed group (treated with 100 mM NaCl and 100 ppm Pb), and groups sprayed with nanoparticles (NPs) at the two concentrations. The treatments involving the nanoparticles were conducted 15, 25 and 40 days following the sowing. The plant samples were then harvested after 45 days to be analyzed in terms of morphological and biochemical parameters.

Photosynthetic pigments assays: In order to measure the carotenoid and chlorophyll (a, b, and total a + b) as recommended by Smith (2013), researchers homogenized 1 g of fresh foliage in 100 mL of an 80% acetone solution. The clarified filtrate was measured in terms of spectrophotometry after filtering the suspension through Whatman No. 1 filter

paper. Measurements of absorbance at 665 nm, 649 and 470 nm were taken to measure the extraction performance and obtain the total pigment yields in strict compliance with the Vernon & Seely (2014) paradigm.

Determination of total soluble carbohydrates and proteins: In order to determine the total amount of soluble carbohydrates, researchers used the classical anthrone sulfuric acid test described by Umbriet *et al.,* (1959). At the same time the analysis of total soluble protein concentrations was done based on the Bio-Rad protein assay following the protocol of the Lowery *et al.,* (1951) to the letter. In both these biochemical studies, researchers measured the required readings of absorbance using one UV-vis spectrophotometer (UNICO model Vis 1200, USA).

Free proline: To evaluate free proline concentrations, investigators implemented the established protocol from Bates *et al.,* (1973). Initially, a homogenate consisting of 0.5 g of desiccated plant tissue and 10 mL of 3% sulfosalicylic acid was passed through Whatman No. 2 filter paper. Concurrently, a specialized ninhydrin reagent was formulated by dissolving 1.25 g of ninhydrin into a chilled blend of 6 M phosphoric acid (20 mL) and glacial acetic acid (30 mL). The core colorimetric assay required mixing 2 mL aliquots of the filtered extract, the prepared ninhydrin reagent, and glacial acetic acid. This solution was incubated in a boiling water bath for 60 minutes, then abruptly halted via an ice bath. To isolate the chromophore, 4 mL of toluene was introduced, followed by vigorous agitation for 15 to 20 seconds. Once the upper organic layer equilibrated to ambient temperature, absorbance was recorded at 520 nm using a UNICO Vis Model 1200 spectrophotometer (USA). Final proline levels were calculated as milligrams per gram of dry weight (mg/g D.Wt.).

Assays of enzymatic antioxidant activities: In order to extract active enzymatic fraction, the researchers used the extraction procedure described by Mukherjee & Choudhuri (1983). The extraction was initiated by placing precisely 2 g of target botanical samples, i.e. terminal buds and the first two young leaves in 10 mL of a 0.1 M phosphate buffer (pH 6.8). The suspension was then centrifuged at 20 000 rpm and 20 minutes in a refrigerated centrifuge at 2°C. The distinct clear supernatant that was obtained in this step served as the main enzyme extract in all further analytical considerations.

Catalase (CAT): Aebi (1983) applied spectrophotometry to establish the catalase (CAT) activity through the drop in the absorbance of the water at 240 nm over 60 seconds. The sample extract was added to a buffer solution consisting of 100 mM potassium phosphate (pH 7.0), 15 mL of water, and 3 mL of 50 µL of the sample extract in total. One unit of enzyme activity was defined as the amount of enzyme required to decompose half of the water in 60 seconds at 25°C.

Peroxidase (POX): In order to effectively measure the activity of peroxidase using the Bergmeyer *et al.,* (1974) model, the authors mixed 0.2 mL of the isolated enzyme extract with 2 mL of 20 mM H_2O_2 and 5.8 mL of 50 mM phosphate buffer solution at pH 7.0. A UV spectrometer was used to measure the enzymatic reaction spectrophotometrically (absorbance values) at different wavelengths (up to 470 nm) that signified the oxidation of pyrogallol over a 60-second time interval at 25°C.

Polyphenol oxidase (PPO): In order to measure the activity of polyphenol oxidase, researchers used the standard Kar and Mishra (1976) procedure. The substrate of the assay was 0.1 M catechol in 0.1 M sodium acetate buffer at pH 5.0. The enzymatic reactions were incubated in 60 minutes at 30°C and an UltraSpec 2000 spectrophotometer monitored the rise in absorbance at 395 nm. Ultimately, these activity computations were expressed as the shift in optical density per minute per gram of fresh weight (OD min^{-1} g^{-1} FWt).

Determination of plant heavy metal contents: Parkinson & Allen's (1975) techniques were followed in order to quantify the lead levels in edible sections of different plant sample matrices. 1 g of dried plant material and 7.5 mL of concentrated sulfuric acid (H_2SO_4) were added to digestion tubes. 7.5 mL of 30% H_2O_2 was added after a 30-minute equilibration time at room temperature. Thermal digestion was then carried out on a hot plate at 360°C for 40 minutes. Once it had cooled to room temperature, 1-mL aliquots were added until the digestion was entirely clear; deionized distilled water was used to standardize the solution's final volume to 50 mL. Whatman No. 42 filter paper was used to finish the filtration process, and Perkin-Elmer 3100 atomic absorption spectrophotometry was used to measure the lead content.

Antimicrobial test of NPs

Option A: The well diffusion method was employed to evaluate how Se and Se/CuO nanoparticles inhibit six specific pathogens. This screening panel consisted of *Salmonella typhi* (ATCC 6539), *Bacillus subtilis* (ATCC 6633), *Staphylococcus aureus* (ATCC 6538), *Escherichia coli* (ATCC 8739), *Penicillium glabrum* (Op694171), and *Candida albicans* (ATCC 10221). Investigators prepared the growth environments by propagating the fungal isolates on potato dextrose agar, whereas they cultivated the bacterial strains on nutrient agar. Researchers created 6-mm radius wells within the cultured agar using a conventional cork borer, subsequently filling each depression with a 25 mg/mL nanoparticle suspension. Experimental baseline was based on DMSO as negative control and Nystatin and Ampicillin as positive control of the fungal and bacterial cultures, respectively. Lastly, the scientists measured the resulting areas of inhibition by keeping fungi at 30°C over a period of five days and keeping bacteria at 37°C over a period of 24 hours (Abd-ElGawad *et al.,* 2025).

Antioxidant assessment of NPs: The capacity of NPs to scavenge DPPH radicals was systematically evaluated. DPPH was dissolved in methanol, while high-purity H2O (Milli Q H_2O) was combined with varying double-fold concentrations of the test substances, spanning a range from 1000 to 1.95 µg mL^{-1}. Within individual test tubes, one ml of each concentration was mixed with 450

microliters of Tris-HCl buffer (pH = 7.4) alongside 1 mL of DPPH solution. Following thorough mixing of tube contents, samples underwent agitation (150 rpm) for a period of 30 minutes at 37°C under dark conditions (Selim *et al.,* 2025). Ascorbic acid at equivalent concentrations functioned as the positive control, whereas the negative control comprised a test tube containing the complete reagent mixture with the exception of the test compounds (either ascorbic acid or NPs).

Statistical analysis

In order to analyze the quantitative information, scientists used one-way analysis of variance (ANOVA) and determined that the significance level of 0.05 was significant. These statistical analyses were based on the computational framework that was based on the Microsoft Excel version 365 and the Statistical Package of the Social Sciences version 25.00 (SPSS v.25) which was used extensively in their completion.

Results and Discussion

Characterization of Se and Se/CuO NPs: In this study, selenium nanoparticles (Se NPs) and selenium/copper oxide nanoparticles (Se/CuO NPs) were prepared using aqueous extracts of spearmint leaves as reducing agents. The use of natural, non-toxic, affordable, and eco-friendly materials as coating agents is the foundation of the eco-friendly synthesis techniques. Color changes in the solution, either dark red (selenium nanoparticles) or dark green (selenium/copper oxide nanoparticles), successfully verified the creation of nanoparticles. The selenium nanoparticles or selenium/copper oxide nanoparticles were nearly monodisperse, spherical, and subspherical in shape, with sizes ranging from 18 to 49 nm for selenium nanoparticles and from 18 to 62 nm for selenium/copper oxide nanoparticles, according to high-resolution electron microscopy (HRTEM) images (Fig. 1).

Morphological analysis revealed that the synthesized spherical, crystalline selenium (Se) and copper oxide (Se/CuO) nanoparticles possessed average diameters of 34.1 nm and 33.8 nm, respectively. To understand the metal precursor reduction mechanisms driving this synthesis, we utilized Fourier transform infrared (FT-IR) spectroscopy to characterize the surface functional groups (Fig. 2). Spectral data highlighted distinct peaks at 3386 and 3417 cm^{-1}, corresponding to O–H bending vibrations characteristic of phenolic compounds. According to Pasieczna-Patkowska *et al.,* (2025), amides' carbonyl C=O functional groups are visible at 1637 cm^{-1}. The vibrations of the alkyl group (OH) functionalities were extended and appeared at 1112 and 1136 cm^{-1} as peaks. The stretching vibrations of the alkyl (OH) group were observed in the form of peaks of 1112 and 1136 cm^{-1}. The stretching vibrations of copper oxide (CuO) or selenium nanoparticles were suggested by the existence of peaks at 621 and 515 cm^{-1}, respectively. Various macromolecules contained in the plant extract, i.e., carbohydrates, amino acids, proteins, and amines, are probably the major mediating functional groups that reduced, capped, and stabilized the selenium and selenium/copper oxide nanoparticles (Nguyen *et al.,* 2023). After this biosynthesis through Mentha viridis leaf extract, the structure of the produced nanomaterials was conclusively assessed by means of powder XRD. The diffraction patterns depicted in Fig. 3 had a distinct and sharp peak as shown. This crystallographic signature is not only a confirmation of the successful creation of the Se NPs, but also a solid confirmation of the highly crystalline character of the populations of both the Se and the Se/CuO nanoparticles (Salem *et al.,* 2021). Sharp, distinct peaks observed within the diffraction pattern indicated that the synthesized Se NPs possessed a highly crystalline structure.

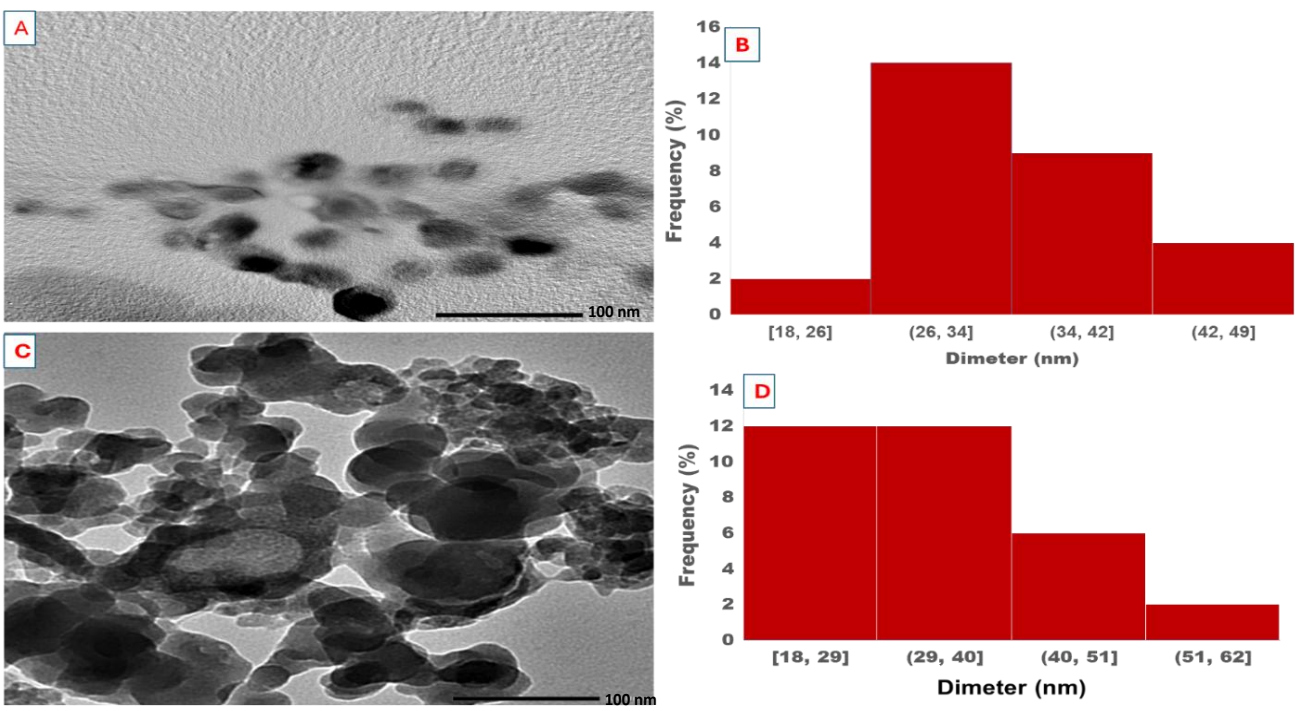

Fig. 1. HRTEM imaging of Se NPs (A), Se/CuO NPs (C), and Particle size and distribution of Se NPs (B), and Se/CuO NPs (D).

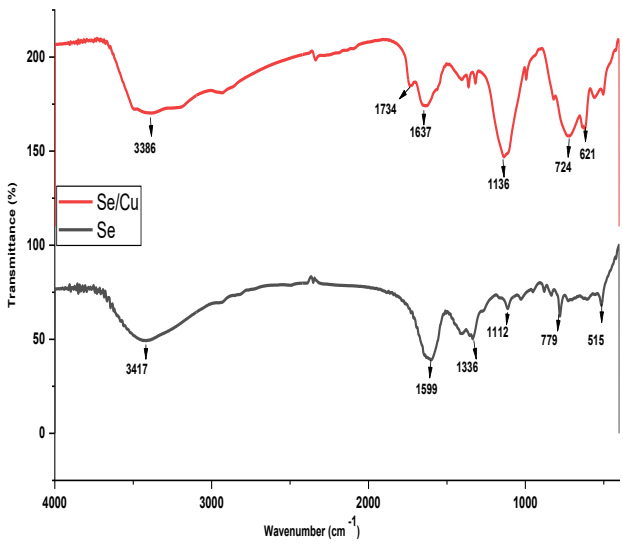

Fig. 2. FTIR of synthesized Se and Se/CuO NPs.

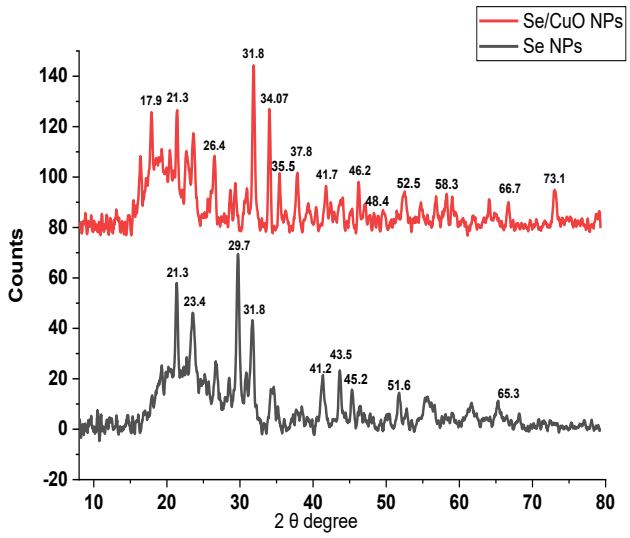

Fig. 3. X-Ray diffraction profile of synthesized Se NPs and Se/CuO NPs.

Table 1. Key words of treatments.

Treatments	Salinity	HM	NPs
Control	-	-	-
S+HMs	100 mM	100 ppm	-
Se 50	-	-	50 ppm
Se 100	-	-	100 ppm
Se/CuO 50	-	-	50 ppm
Se/CuO 100	-	-	100 ppm
Se 50 + S + HMs	100 mM	100 ppm	50 ppm
Se 100 + S + HMs	100 mM	100 ppm	100 ppm
Se/CuO + S+ HMs	100 mM	100 ppm	50 ppm
Se/CuO + S + HMs	100 mM	100 ppm	100 ppm

At angles of 23.4o, 29.7o, 41.2o, 43.5o, 45.2o, 51.6o, and 65.3o, which corresponded to crystal planes (100), (101), (110), (102), (111), (201), and (210), respectively, the 20 values in the XRD pattern ranged from 10° to 80° (JCPDS card No. 06-0362) (Cruz *et al.,* 2019). The Se/CuO nanocomposite XRD revealed a set of CuO NP diffraction peaks at 35.5o (002), 37.8o (111), 48,4o (220), 52.5o (211), 58.3o (202), 66.7o (022), and 73.1o (311) of the face-centered monoclinic and cubic planes of CuO NPs (JCPDS Nos 00-005-0667) (Okpara *et al.,* 2021). XRD pattern analysis showed that the produced selenium and selenium/copper oxide nanoparticles had crystalline characteristics.

Clover plant growth characteristics in response to varying Se and Se/CuO NP applications: Environmental stressors such as salinity and heavy metal contamination disrupt water uptake and induce premature senescence and photosynthetically active leaf surface area reduction, resulting in reduced growth rates, osmotic disturbances, and nutritional imbalance (Sairam & Tyagi, 2004). Table 2 shows that applications of selenium or selenium-copper oxide nanoparticle are critical in saline conditions (100 mM) and heavy metal contamination (100 ppm lead) on morphological parameters (shoot and root elongation and fresh and dry biomass accumulation in the shoot and root).

Application of Se/CuO NP at 50 ppm yielded the most substantial improvements in shoot and root elongation as well as the greatest fresh and dry weight accumulation for both plant structures. Upon penetration into plant tissues, nanoparticles engage with cellular and subcellular machinery, triggering modifications of a structural, biochemical, biological, and genetic nature. The nature of these effects, whether advantageous or detrimental, varies according to the specific nanoparticle type and plant species under consideration (Khan *et al.,* 2019). The way in which nanoparticles impact plant systems is affected by several determinants: their chemical composition, their reactivity, their size, and their concentration on external surfaces or within internal tissues (Zulfiqar & Ashraf, 2021). Notably, stress-exposed groups documented in Table 2 exhibited the poorest performance across all morphological characteristics examined values that fell below both control conditions and every applied treatment.

Table 2. Effect of Se, Se/CuO NPs on morphological characterization of clover plants under stress conditions. Each value is mean of 8 replicates ± the standard error of means.

Treatments		Shoot lengths (cm)	Root lengths (cm)	Fresh weight of shoot	Fresh weight of root	Dry weight of shoot	Dry weight of root
Control	0 ppm	14.33 ± 1.26ab	4.67 ± 0.58ab	0.586 ± 0.11cde	0.14 ± 0.03ab	0.04 ± 0.01bcd	0.04 ± 0.01ab
S+HM	100 mM 50 ppm	8.33 ± 1.53b	2.33 ± 0.74b	0.345 ± 0.08e	0.06 ± 0.04b	0.01 ± 0.01d	0.02 ± 0.02b
Se	50 ppm	15.50 ± 1.32a	4.83 ± 0.73ab	0.891 ± 0.19abc	0.15 ± 0.01ab	0.05 ± 0.01bc	0.05 ± 0.02ab
	100 ppm	14.00 ± 1.35ab	5.33 ± 1.53ab	0.950 ± 0.15ab	0.13 ± 0.05ab	0.05 ± 0.02bc	0.05 ± 0.02ab
Se/Cu	50 ppm	16.33 ± 2.52a	6.77 ± 1.04a	1.01 ± 0.18a	0.16 ± 0.09ab	0.09 ± 0.01ab	0.08 ± 0.01ab
	100 ppm	13.50 ± 1.31ab	6.67 ± 0.79a	1.01 ± 0.12a	0.15 ± 0.02a	0.08 ± 0.02a	0.06 ± 0.02a
Se + S + HM	50 ppm	11.33 ± 1.55ab	4.17 ± 0.76ab	0.42 ± 0.06e	0.12 ± 0.01ab	0.02 ± 0.01d	0.03 ± 0.01ab
	100 ppm	13.00 ± 3.46ab	4.67 ± 2.08ab	0.66 ± 0.07bcde	0.11 ± 0.01ab	0.03 ± 0.01cd	0.04 ± 0.01ab
Se/Cu + S + HM	50 ppm	12.00 ± 2.65ab	4.50 ± 1.32ab	0.54 ± 0.09de	0.12 ± 0.03ab	0.03 ± 0.01cd	0.04 ± 0.01ab
	100 ppm	12.33 ± 1.53ab	4.83 ± 0.29ab	0.83 ± 0.09abcd	0.14 ± 0.04ab	0.03 ± 0.01bcd	0.04 ± 0.01ab

Photosynthetic pigments of clover plants under different treatments: The promotion role of Se and Se/CuO NPs at different doses on chlorophyll a, b and a+b appeared under stress conditions is shown in Fig. 4. The lowest values of pigment contents were caused by Salinity and Pb stress. There is a good body of literature that shows physiological deterioration caused by salinity, e.g., when plants are exposed to 200 mM NaCl, photosynthetic rates are significantly inhibited within the first three days of the stress (Abogadallah, 2010). Although the saline environment usually reduces the concentration of chlorophyll and carotene in leaf, the recent study of Gonzalez-Garcia *et al.,* (2021) indicates that nanotechnology is protective against saline conditions in Capsicum annuum. Precisely, exogenous addition of Se NPs (10 and 50 mg L^{-1}) or Cu NPs (100 and 500 mg L^{-1}) was effective in enhancing these crucial photosynthetic pigments to overcome the degradation impact of salt stress. Saline stress simultaneously causes osmotic stress to the plants, hence restricting the supply of water and ultimately dehydrating the cells and turgor loss. Also, ionic toxicity and nutritional imbalance are induced, excess generation of ROS is augmented, all which may be perilous and detrimental radicals, capable of oxidatively impairing lipids, proteins, and DNA (Kamanga *et al.,* 2020). On the other hand, NPs show the ability to increase chlorophyll levels, hence lowering the ROS content, and increasing photochemical activity. Besides, NPs have positive impacts on particular chloroplast enzymes involved in the synthesis of photosynthetic pigments (Siddiqui *et al.,* 2014).

Hussein *et al.,* (2019) reported enhanced chlorophyll concentrations in peanut crops following Se NP application. Similarly, the administration of Cu NPs at 2.5 mg L^{-1} resulted in a 50% elevation in carotenoid levels (lutein, violaxanthin, and beta-carotene) within Oryza sativa (Da Costa & Sharma 2016).

Carbohydrates, protein, and proline contents: Exposure to salinity and lead stress conditions led to marked reductions in soluble carbohydrate and protein levels (Fig. 5). Conversely, application of Se either independently or in the form of Se/CuO NPs across various concentrations produced substantial elevations in these critical metabolites relative to the stress-treated groups. Maximum carbohydrate accumulation was observed under Se/CuO NP treatment at 100 ppm. Stress imposition in our experimental system induced a high increase in proline.

Wan *et al.,* (2020) investigated other nanoparticle formulations and found that carbon-based nanoparticles increased root fresh biomass, soluble sugar, and total protein levels in *Sophora alopecuroides* seedlings exposed to saline conditions. Comparable findings were reported by Shafiq *et al.,* (2019), wherein the use of polyhydroxy fullerene nanoparticles for seed priming purposes mitigated salt stress effects in germinating wheat seedlings through enhanced amino acid biosynthesis and elevated soluble sugar reserves. Additionally, protein accumulation was augmented in *Triticum sativum* plants treated with silver nanoparticles (Jhanzab *et al.,* 2019).

Enzymes activity and Pb content in response to NPs under stress conditions: The activities of catalase, peroxidase and polyphenol oxidase (Fig. 6) were significantly enhanced by saline exposure as well as lead contamination, while accumulation of malondialdehyde was increased in clover leaf tissue exposed to stress factors; however, the lowest expression of antioxidant enzymes under stressful conditions occurred with application of Se/CuO NPs at a concentration of 100 ppm compared with control and stressed groups without nanoparticle treatment. When plants were not subjected to any kind of environmental challenge (non-stressed), selenium nanoparticles or selenium-copper oxide nanoparticles only showed slight increases in most measured parameters when compared with controls. Nanoparticles characteristically amplify enzymatic antioxidant machinery responsible for neutralizing reactive oxygen species-particularly ascorbate peroxidase, superoxide dismutase, catalase, and monodehydroascorbate reductase (Hossain, *et al* 2020).

Surface characteristics such as dimensional parameters, morphological configuration, and porosity influence both surface charge distribution and free energy properties. The significance of these attributes lies in the fact that nanoparticle-plant interactions are initiated at the cellular interface, subsequently initiating a series of physiological responses. The translations of these responses include causing the production of biomarkers of stress that trigger defensive pathways in the plant system. This in turn causes the production of enzymatic antioxidants and accumulation of non-enzymatic antioxidants both of which increase the activity of antioxidant enzymes. This improvement eventually reduces oxidative stress caused on the structures of the membranes and enhances increment of salt (Zhu *et al*., 2004).

Heavy metal contamination poses significant challenges to agricultural productivity and threatens global food security. Here we found extremely high lead concentrations (up to 2,000% over controls) under stress conditions that nanoparticle treatments significantly reduced (Fig. 7). The most substantial mitigation occurred following Se/CuO NP administration at 50 ppm—a treatment that suppressed lead accumulation by 25.12 percent relative to stressed plants receiving no nanoparticle amendment. Comparable protective effects have been documented in carrot cultivation systems where wastewater irrigation was employed; selenium nanoparticle supplementation in that context diminished tissue concentrations of nickel, cadmium, and lead (El-Batal *et al.,* 2023).

Antimicrobial and antioxidant properties of Se and Se/CuO NPs: As visualized in Fig. 8, the bimetallic Se/CuO composites exhibited antimicrobial properties that consistently outperformed both the baseline control and the standalone Se nanoparticles. Table 3 quantifies these distinct zones of clearance. Rather than listing independent sequences, direct comparisons reveal the enhanced suppressive power of Se/CuO over Se alone against specific pathogens: *E. faecalis* (40±0.2 vs. 30±0.4 mm), *S. aureus* (19±0.1 vs. 15±0.2 mm), *K. pneumonia* (27±0.5 vs. 23±0.5 mm), and *S. typhi* (26±0.6 vs. 21±0.3 mm). Similar enhanced efficacy was observed against *C. albicans* (32±0.4 vs. 28±0.1 mm) and *M. circinelloid* (30 vs. 13 mm). Significant variations in clearance halos emerged upon evaluating the suppressive capabilities of bimetallic Se/CuO against monometallic Se formulations, as well as standard pharmacological treatments. Corroborating this enhanced synergistic efficacy, recent literature highlights similar multi-metal advantages; for instance, Qanash *et al.,* (2024) demonstrated that doping zinc oxide with selenium nanoparticles amplified biocidal reach across diverse fungal and bacterial strains. To prevent sequential pattern matching, their recorded suppression radii can be paired directly with the targets: *S. aureus* (28.33 mm), *B. subtilis* (27.33 mm), *B. cereus* (27.67 mm), *P. aeruginosa* (27.17 mm), *E. coli* (27.5 mm), *S. typhi* (24.33 mm), *C. albicans* (23.33 mm), and *Aspergillus niger* (18.17 mm). Furthermore, standalone Se

nanoparticles exhibit established toxicity against *B. subtilis*, *S. aureus*, *K. pneumoniae*, *C. albicans*, and *E. coli* (Alghonaim *et al.,* 2024). Abd-ElGawad *et al.,* (2025) further checked the augmented potency of the Se/CuO composite which was synthesized through an extract of Urtica urens by comparing it with a similar microbial spectrum. Lastly, the radical scavenging analyses revealed the enhanced antioxidant ability of the bimetallic construct compared to that of pure Se (Table 4). The bimetallic Se/CuO nanoparticles measured 8.19 ± 0.49 µg/mL in IC50, which is much higher than that of the monometallic Se nanoparticles (23.68 ± 0.19 µg/mL). To put the data in context, the positive standard, ascorbic acid, gave a baseline of 3.21 ± 1.22 µg /mL. This bimetallic potency is a sharp contrast to other studies carried out by Dulta *et al.,* (2022), which revealed a much lower active IC50 of 91.2 ug/mL of pure CuO nanoparticles. These differences in scavenging potential are usually determined by the botanical intermediates that mediate the synthesis. Peddi *et al.,* (2021) illustrated this biological influence: whereas the raw sea sedge extract yielded an IC50 of 51.71 µg/mL, the CuO nanoparticles derived from this identical plant source displayed an enhanced concentration of 28.05 µg/mL. According to Peddi *et al.,* (2021), the IC50 value for copper oxide nanoparticles derived from plants was 28.05 µg/ml, whereas the IC50 value for sea sedge, the plant source employed in their production, was 51.71 µg/ml.

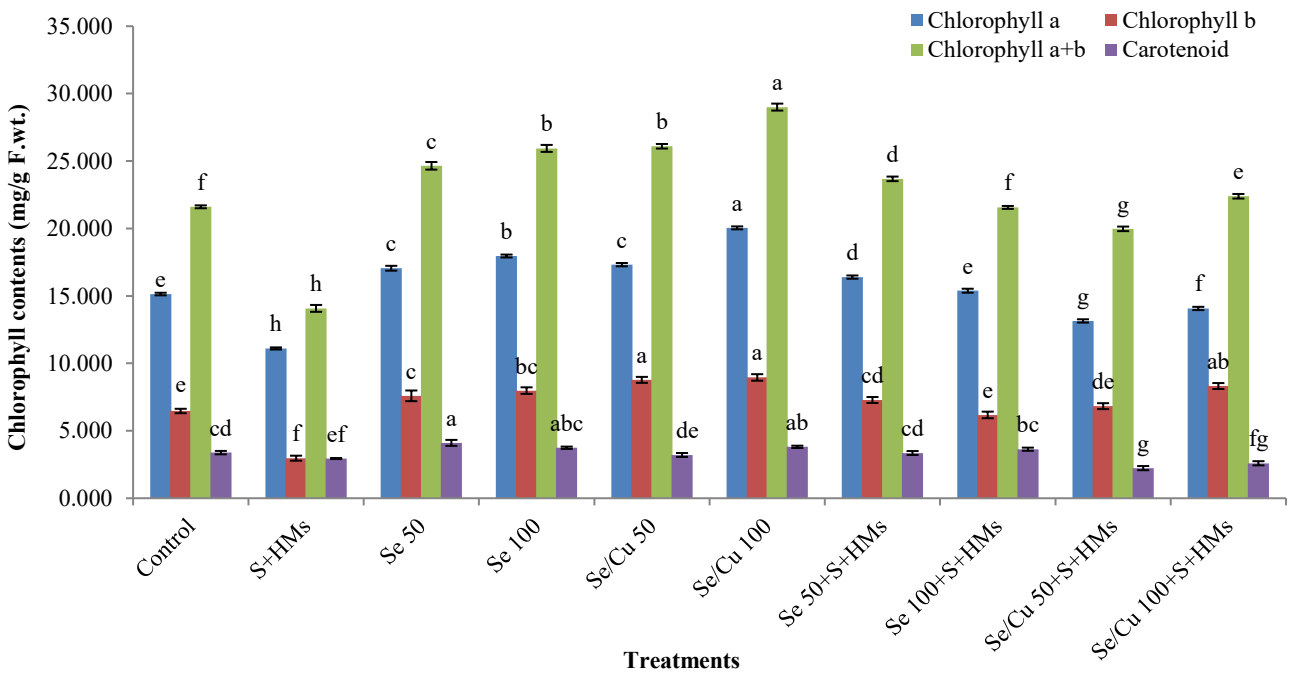

Fig. 4. Effect of Se or Se/CuO NPs on photosynthetic pigments of clover plants under stress conditions. Each value is mean of 3 replicates ± the standard error of means.

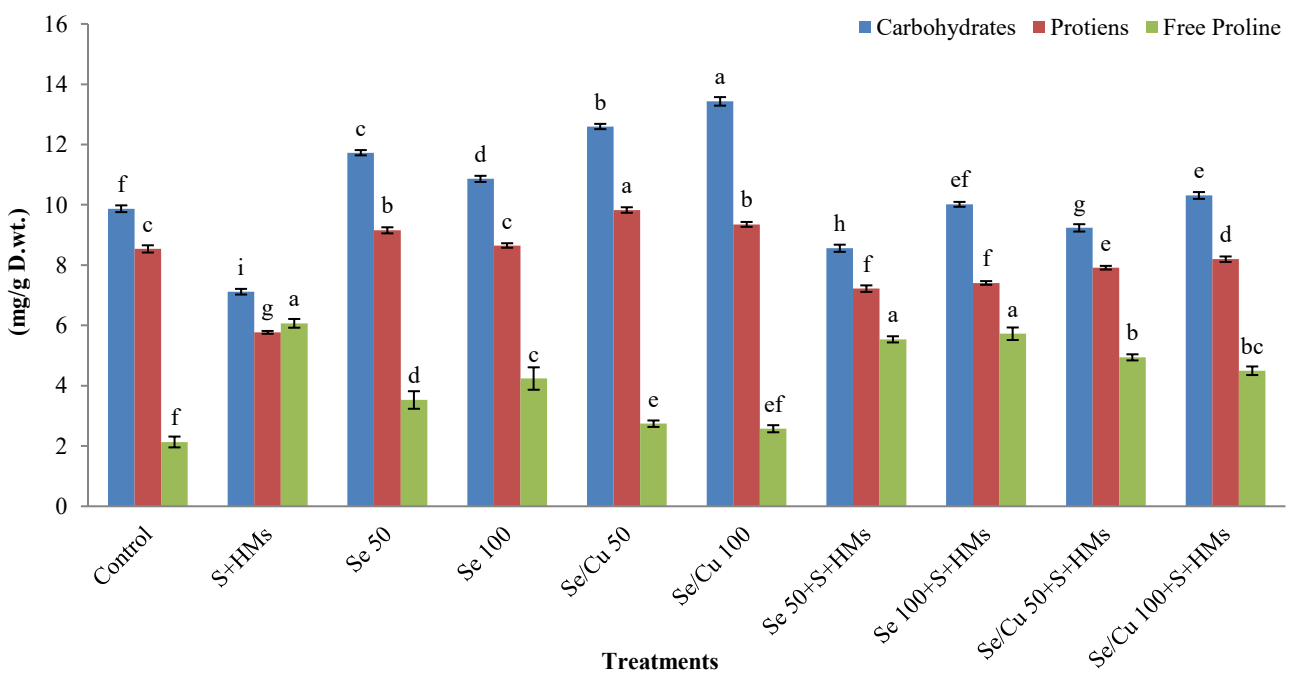

Fig. 5. Carbohydrates, protein, and proline contents of clover plants under different treatments. Each value is mean of 3 replicates ± the standard error of means.

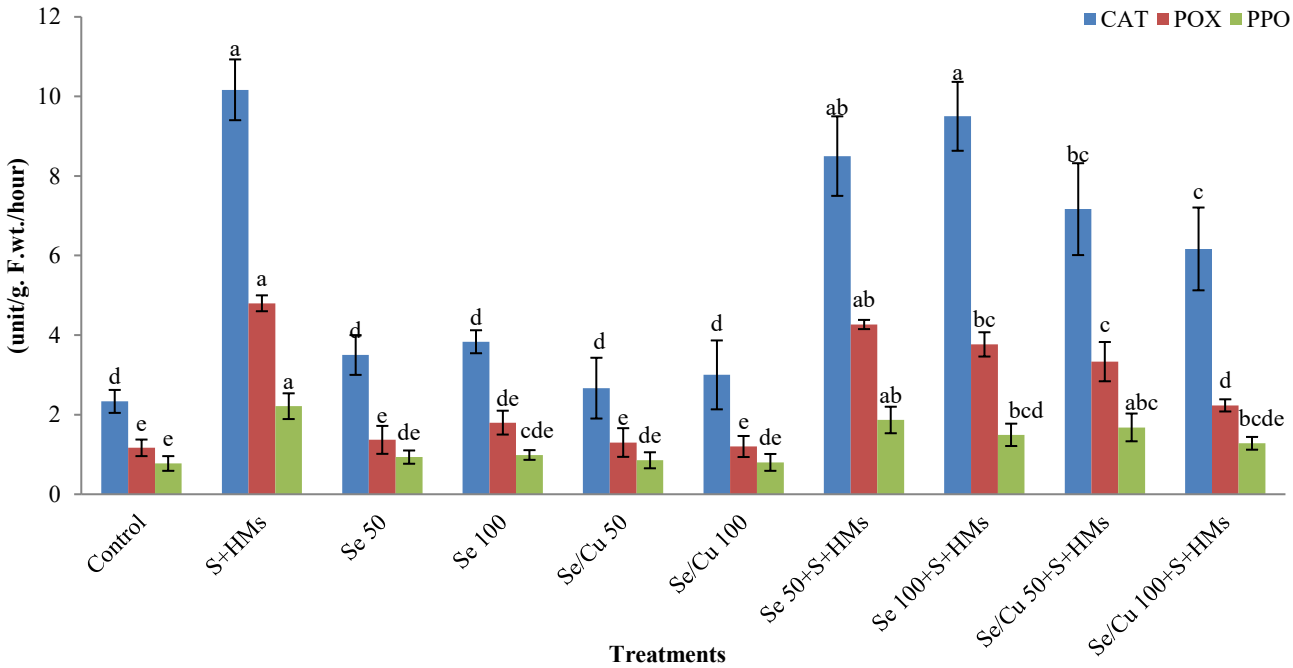

Fig. 6. Antioxidant enzymes activity of clover plants under different treatments of NPs under normal and stress conditions. Each value is mean of 3 replicates ± the standard error of means.

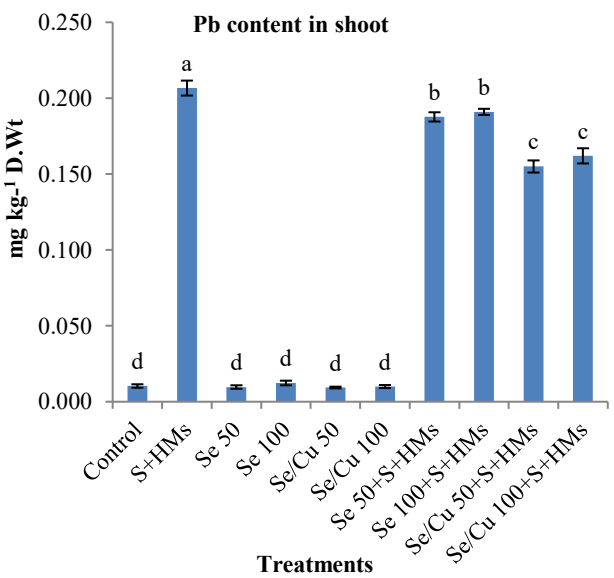

Fig. 7. Effect of Se or Se/CuO NPs on Pb contents of clover plants under normal and stress conditions. Each value is the mean of 3 replicates ± the standard error of means.

Table 3. Effectiveness of SeNPs and Se/ CuO NPs versus checked microbes.

Tested microorganisms	Mean Inhibition Zone (mm)				HSD
	Se NPs	Se/CuO NPs	+ve C*	-ve C*	
E. faecalis	30 ± 0.4	40 ± 0.2	21 ± 0.4	0.0	2.27
S. aureus	15 ± 0.2	19 ± 0.1	16 ± 0.1	0.0	1.06
K. pneumonia	23 ± 0.5	27 ± 0.5	20 ± 0.5	0.0	1.27
S. typhi	21 ± 0.3	26 ± 0.6	20 ± 0.2	0.0	1.65
C. albicans	28 ± 0.1	32 ± 0.4	15 ± 0.2	0.0	2.21
M. circinelloid	13	30	24 ± 0.2	0.0	2.36

Table 4. Antioxidant properties of selenium nanoparticles and selenium/CuO nanoparticles.

Concentration (µg/mL)	DPPH scavenging (%)			HSD at 0.05
	Se NPs	Se/CuO NPs	Ascorbic	
1.95	20.7 ± 0.25c	34.7 ± 0.23b	43.0±0.08a	3.02
3.9	28.3 ± 0.15c	39.7 ± 0.36b	50.2 ± 0.18a	1.03
7.8125	36.8 ± 0.36c	48.1 ± 0.25b	56.3 ± 0.29a	2.03
15.625	45.0 ± 0.21c	56.8 ± 0.65b	65.4 ± 0.43a	4.03
31.25	53.3 ± 0.01c	65.0 ± 0.46b	74.5 ± 0.64a	1.02
62.5	61.9 ± 0.02c	73.7 ± 0.46b	81.8 ± 0.15a	1.02
125	70.1 ± 0.09c	83.2 ± 0.49b	89.0 ± 0.36a	1.36
250	78.7 ± 0.18c	89.3 ± 0.38b	93.0 ± 0.39a	2.03
500	86.9 ± 0.36b	92.1 ± 0.48a	95.7 ± 0.16a	4.03
1000	91.4 ± 0.15b	96.0 ± 0.98a	98.5 ± 0.18a	2.65
IC_{50} (µg/mL)	23.68 ± 0.19a	8.19 ± 0.49b	3.21 ± 0.122c	0.98

Conclusion

Selenium (Se) and bimetallic selenium/copper oxide (Se/CuO) nanoparticles were used to mitigate salinity and heavy metal stressors in clover plants successfully. The present study has shown that the given nanomaterials have significantly increased the soluble carbohydrates and protein levels, as well as promoted pigment formation and morphological growth parameters. This physiological stress alleviation, which occurred in a mechanical manner, was directly associated with the increase in the activity of antioxidant enzymes and simultaneous reduction in the accumulations of the cellular proline. It is important to note that the 50-ppm level of Se/CuO nanoparticles was found the best dose to maximize the vitality of the plants and reduce lead (Pb) bioaccumulation in unfavorable environmental conditions. On the other hand, the dosage of 100 ppm was higher in order to maximize the carbohydrate and protein yields during stressful periods. Moreover, the bimetallic Se/CuO sample was found to have better antimicrobial properties against a range of pathogens such as S. aureus, E. faecalis, K. pneumoniae, S. typhi, C. albicans and M. circinelloid than the monometallic Se nanoparticles with both formulations having strong free-radical scavenging abilities.

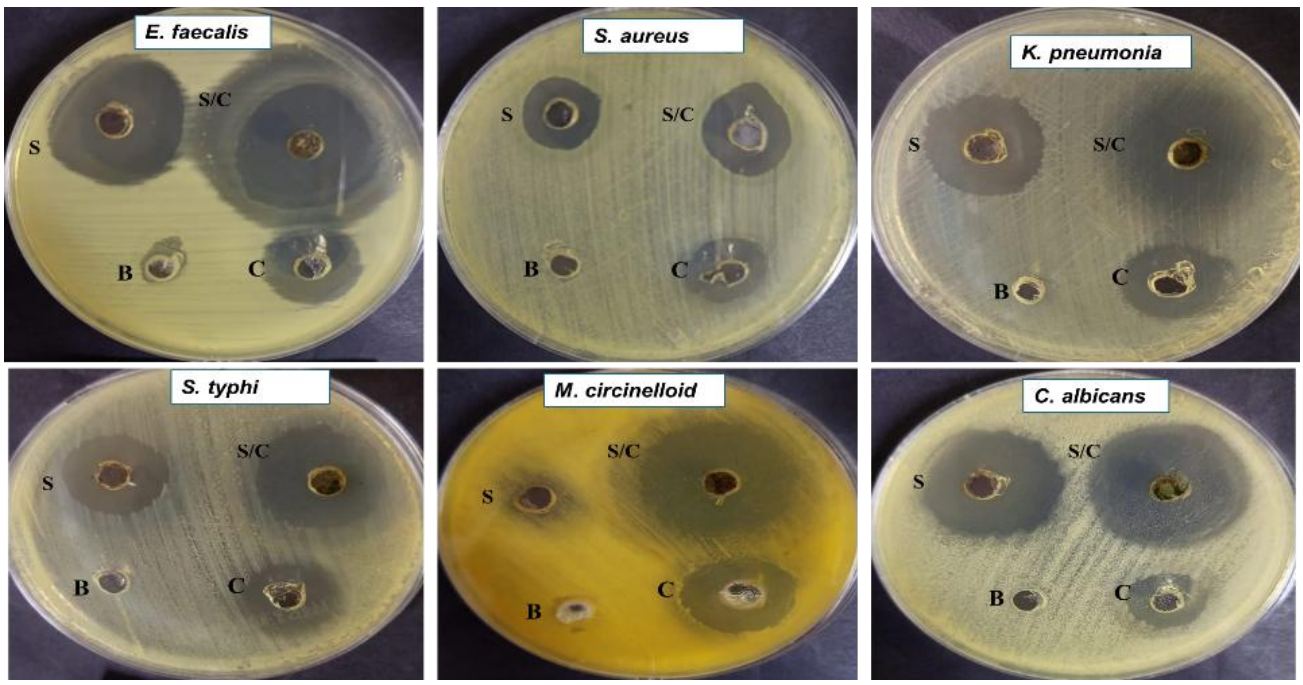

Fig. 8. Efficacy of *Se NPs and* Se/CuO NPs against tested microorganisms (S, *Se NPs*; S/C, Se/CuO NPs; C, positive control; S, solvent used as negative control).

Conflict of Interest: The authors declare that they have no conflict of interest.

Author's Contribution: Abdelatti I. Nowwar, conceptualization, project administration, methodology, formal analysis, writing original draft. Abeer S. Meganid, conceptualization, methodology, data curation, formal analysis, writing-reviewing and editing. All authors read and approved the final manuscript.

Data Availability: All data generated or analyzed during this study available from the corresponding author on request.

References

Abd-ElGawad, A.M., M.A.A. Amin, M.A. Ismail, M.K. Ismail, A.A. Radwan, T.C. Sarker, A. Medhat, M.A. El-Naggar and E.M. Abdelkareem. 2025. Selenium/copper oxide nanoparticles prepared with urtica urens extract: Their antimicrobial, antioxidant, antihemolytic, anticoagulant, and plant growth effects. *BioResour.*, 20(2): 2791-2810.

Abdelghany, T.M. 2013. *Stachybotrys chartarum*: A novel biological agent for the extracellular synthesis of silver nanoparticles and their antimicrobial activity. *Indones J. Biotechnol.,* 18(2): 75-82. DOI: 10.22146/ijbiotech.7871

Abogadallah, G.M. 2010. Sensitivity of *Trifolium alexandrinum* L. to salt stress is related to the lack of long-term stress-induced gene expression. *Plant Sci.*, 178(6): 491-500.

Aebi, H.E. 1983. Catalase. Methods Enzym. *Anal.*, 105: 121-126.

Alghonaim, M.I., S.A. Alsalamah, Y. Ali and T.M. Abdelghany. 2024. Green mediator for selenium nanoparticles synthesis with antimicrobial activity and plant biostimulant properties under heavy metal stress. *Bio. Resources*, 19(1): 898-916.

Al-Rajhi, A.M., S. Selim, A.E. Abdalla, N. Hagagy, A.A.N. Saddiq, S.K. AlJaouni and T.M. Abdelghany. 2024. Synthesis of chitosan/Fe_2O_3/CuO-nanocomposite and their role as inhibitor for some biological disorders *In vitro* with molecular docking interactions studies. *Int. J. Biol. Macromol.*, 280(1): 135664.

Amin, M.A., N.A. Algamdi, M.S. Waznah, D.A. Bukhari, S.M. Alsharif, F. Alkhayri, M. Abdel-Nasser and A. Fouda. 2025. An insight into antimicrobial, antioxidant, anticancer, and antidiabetic activities of trimetallic Se/ZnO/CuO nanoalloys fabricated by aqueous extract of *Nitraria retusa. J. Cluster Sci.,* 36(1): 1-15. DOI:10.1007/s10876-024-02742-6

Amin, M.A.A., A.M. Abu-Elsaoud, A.I. Nowwar, A.T. Abdelwahab, M.A. Awad, S.E.D. Hassan and A. Elkelish. 2024. Green synthesis of magnesium oxide nanoparticles using endophytic fungal strain to improve the growth, metabolic activities, yield traits, and phenolic compounds content of *Nigella sativa* L. *Green Proce. Synth.*,13(1): 20230215. DOI:10.1515/gps-2023-0215

Atta, K., S. Mondal, S. Gorai, A.P. Singh, A. Kumari, T. Ghosh and D. Jespersen. 2023. Impacts of salinity stress on crop plants: improving salt tolerance through genetic and molecular dissection. *Front. Plant Sci.*, 14: 1241736. https://doi.org/10.3389/fpls.2023.1241736

Bates, L.S., R.P Waldren and I.D. Teare. 1973. Rapid determination of free proline for water-stress studies. *Plant Soil*, 39: 205-207.

Bergmeyer, H.U., K. Gawehn and M. Grassl. 1974. Methods of Enzymatic Analysis. Bergmeter HU, ed. *Acad Press New York*, 3: 1205-1215.

Cruz, L. Y., D. Wang and J. Liu. 2019. Biosynthesis of selenium nanoparticles, characterization and X-ray induced radiotherapy for the treatment of lung cancer with interstitial lung disease. *J. Photochem. Photobiol. B: Biology*, 191: 123-127.

Da Costa, M.V.J. and P.K. Sharma. 2016. Effect of copper oxide nanoparticles on growth, morphology, photosynthesis, and antioxidant response in *Oryza sativa*. *Photosynthetica*, 54: 110-119.

Das, A. and B. Das. 2019. Nanotechnology a potential tool to mitigate abiotic stress in crop. *Abiotic and biotic stress in plants*, 85.

Dulta, K., A.G. Koşarsoy, P. Chauhan, R. Jasrotia, P.K. Chauhan and J.O. Ighalo. 2022. Multifunctional CuO nanoparticles with enhanced photocatalytic dye degradation and antibacterial activity. *Sustain. Environ. Res.*, 32(1):2. https://doi.org/10.1186/s42834-021-00111-w

El-Batal, A.I., M.A. Ismail, M.A. Amin, G.S. El-Sayyad and M.S. Osman. 2023. Selenium nanoparticles induce growth and physiological tolerance of wastewater-stressed carrot plants. *Biologia,* 78(9): 2339-2355.

Elkady, F.M., B.M. Badr, E. Saied, A.H. Hashem, M.A. Abdel-Maksoud, S. Fatima and H.R. Hashem. 2025. Green biosynthesis of bimetallic copper oxide-selenium nanoparticles using leaf extract of *Lagenaria siceraria*: Antibacterial, anti-virulence activities against multidrug-resistant pseudomonas aeruginosa. *Int. J. Nanomed.*, 4705-4727.

González-García, Y., C. Cárdenas-Álvarez, G. Cadenas-Pliego, A. Benavides-Mendoza, M. Cabrera-de-la-Fuente, A. Sandoval-Rangel, J. Valdés-Reyna and A. Juárez-Maldonado. 2021. Effect of three nanoparticles (Se, Si and Cu) on the bioactive compounds of bell pepper fruits under saline stress. *Plants*, 10: 217.

Hossain, Z., F. Yasmeen and S. Komatsu. 2020. Nanoparticles: synthesis, morphophysiological effects, and proteomic responses of crop plants. *Int. J. Mol. Sci.*, 21(9): 3056.

Hussein, H.A.A., O.M. Darwesh and B.B. Mekki. 2019. Environmentally friendly nano-selenium to improve antioxidant system and growth of groundnut cultivars under sandy soil conditions. *Biocatal. Agri. Biotechnol.*, 18: 101080.

Jhanzab, H.M., A. Razzaq, Y. Bibi, F. Yasmeen, H. Yamaguchi, K. Hitachi, K. Tsuchida and S. Komatsu. 2019. Proteomic analysis of the effect of inorganic and organic chemicals on silver nanoparticles in wheat. *Int. J. Mol. Sci.*, 20(4): 825. DOI: 10.3390/ijms20040825

Juárez-Maldonado, A., G. Tortella, O. Rubilar, P. Fincheira and A. Benavides-Mendoza. 2021. Biostimulation and toxicity: The magnitude of the impact of nanomaterials in microorganisms and plants. *J. Adv. Res.*, 31: 113-126.

Kamanga, R.M., K. Echigo, K. Yodoya, A.M.M. Mekawy and A. Ueda 2020. Salinity acclimation ameliorates salt stress in tomato (*Solanum lycopersicum* L.) seedlings by triggering a cascade of physiological processes in the leaves. *Scientia Horticulturae*, 270: 109434.

Kar, M. and D. Mishra. 1976. Catalase, peroxidase, and polyphenoloxidase activities during rice leaf senescence. *Plant Physiol*., 57: 315-319. https://doi.org/10.1104/pp.57.2.315

Kassem, M.E., M.M. Marzouk, A.A. Mostafa, W.K. Khalil and H.F. Booles. 2017. Phenolic constituents of *Trifolium resupinatum* var. *minus*: Protection against rosiglitazone induced osteoporosis in type 2 diabetic male rats. *J. App. Pharm. Sci.*, 7(5): 174-183.

Khalid, M.F., R. Iqbal-Khan, M.Z. Jawaid, W. Shafqat, S. Hussain, T. Ahmed, M. Rizwan, S. Ercisli, O.L. Pop and M.R. Alina. 2022. Nanoparticles: The plant saviour under abiotic stresses. *Nanomaterials*, 12(21): 3915.

Khan, M.R., V. Adam, T.F. Rizvi, B. Zhang, F. Ahamad, I. Jośko, Y. Zhu, M. Yang and C. Mao. 2019. Nanoparticle–plant interactions: two-way traffic. *Small*, 15(37): 1901794.

Lowery, O. H., N.J. Rosebrough, A.L. Farr and R.J. Randall 1951. Protein measurement with the Folin phenol reagent. *J. Biol.. Chem.*, 193(1): 265-275.

Mukherjee, S.P. and M.A. Choudhuri. 1983. Implications of water stress-induced changes in the levels of endogenous ascorbic acid and hydrogen peroxide in *Vigna* seedlings. *Physiol. Plant,* 58:166-170. https://doi.org/10.1111/j.1399-3054.1983.tb04162.x

Nguyen, T.T.T., Y.N.N. Nguyen, , X.T. Tran, T.T.T. Nguyen and T.V. Tran. 2023. Green synthesis of CuO, ZnO and CuO/ZnO nanoparticles using *Annona glabra* leaf extract for antioxidant, antibacterial and photocatalytic activities. *J. Environ. Chem. Engin.,* 11: 111003.

Okpara, E. C., O.E. Ogunjinmi, O.A. Oyewo, O.E. Fayemi and D.C. Onwudiwe. 2021. Green synthesis of copper oxide nanoparticles using extracts of *Solanum macrocarpon* fruit and their redox responses on SPAu electrode. *Heliyon*, 7(12): 1-13.

Parkinson, J.A. and S.E. Allen. 1975. A wet oxidation procedure suitable for the determination of nitrogen and mineral nutrients in biological material. *Commun Soil Sci. Plant Anal.*, 6: 1-11.

Pasieczna-Patkowska, S., M. Cichy and J. Flieger. 2025. Application of Fourier transform infrared (FTIR) spectroscopy in characterization of green synthesized nanoparticles. *Molecules*, 30(3): 684.

Peddi, P., P.R. Ptsrk, N.U. Rani and S.L. Tulasi. 2021. Green synthesis, characterization, antioxidant, antibacterial, and photocatalytic activity of *Suaeda maritima* (L.) Dumort aqueous extract-mediated copper oxide nanoparticles. *J. Gen. Engin. and Biotechnol.,* 19(1): 131.

Qanash, H., A.S. Bazaid, T. Alharazi, H. Barnawi, K. Alotaibi, A.R.M. Shater and T.M. Abdelghany. 2024. Bioenvironmental applications of myco-created bioactive zinc oxide nanoparticle-doped selenium oxide nanoparticles. *Biomass Conver. Biorefin.,* 14(15): 17341-17352.

Safdar, M., S. Aslam, M. Akram, A. Khaliq, S. Ahsan, A. Liaqat, M. Mirza, M. Waqas and W.A. Qureshi. 2023. *Bombax ceiba* flower extract mediated synthesis of Se nanoparticles for antibacterial activity and urea detection. *World J. Microbiol. Biotechnol*., 39(3): 80. DOI: 10.1007/s11274-022-03513-z

Sairam, R.K. and A. Tyagi. 2004. Physiology and molecular biology of salinity stress tolerance in plants. *Curr. Sci.*, 407-421.

Salem, S.S., M.M. Fouda, A. Fouda, M.A. Awad, E.M. Al-Olayan, A.A. Allam and T.I. Shaheen. 2021. Antibacterial, cytotoxicity and larvicidal activity of green synthesized selenium nanoparticles using *Penicillium corylophilum*. *J. Cluster Sci.*, 32: 351-361.

Sampantamit, T., L. Ho, C. Lachat, G. Hanley-Cook and P. Goethals. 2021. The contribution of Thai fisheries to sustainable seafood consumption: national trends and future projections. *Foods*, 10(4): 880.

Selim, S., A.A. Saddiq, R.A. Ashy, A.M. Baghdadi, A.J. Alzahrani, E.M. Mostafa, S.K. AlJaouni, M.Y.M. Elamir, M.A. Amin, A.M. Salah and N. Hagagy. 2025. Bimetallic selenium/zinc oxide nanoparticles: biological activity and plant biostimulant properties. *AMB Express*, 15(1): 1-11.

Shafiq, F., M. Iqbal, M. Ali and M.A. Ashraf. 2019. Seed pre-treatment with polyhydroxy fullerene nanoparticles confer salt tolerance in wheat through upregulation of H_2O_2 neutralizing enzymes and phosphorus uptake. *J. Soil Sci. Plant Nutr.*, 19: 734-742. DOI: 10.1007/s42729-019-00073-4

Siddiqui, M.H., M.H. Al-Whaibi, M. Faisal and A.A. Al Sahli. 2014. Nano-silicon dioxide mitigates the adverse effects of salt stress on *Cucurbita pepo* L. *Environ. Toxicol. Chem.*, 33(11): 2429-2437.

Smith, K.C. 2013. The science of photobiology. *Springer Science & Business Media*. 2nd Ed. 1-47.

Soliman, M.K., M.A. Amin, A.I. Nowwar, M.H. Hendy and S.S. Salem. 2024. Green synthesis of selenium nanoparticles from *Cassia javanica* flowers extract and their medical and agricultural applications. *Sci. Repo.,* 14(1): 26775.

Umbriet, W.W., R.H. Burris, J.F. Stauffer, P.P. Cohen, W.J. Johnse, G.A. Leepage, V.R. Potten and W.C. Schneider. 1959. Manometric Techniques. A manual describing methods applicable to the study of tissue metabolism. *Burgess*, Minneap p. 239.

Vahdati, M. and T.T. Moghadam. 2020. Synthesis and characterization of selenium nanoparticles-lysozyme nanohybrid system with synergistic antibacterial properties. *Sci. Rep*., 10(1): 510. https://doi.org/10.1038/s41598-019-57333-7

Vernon, L.P. and G.R. Seely. 2014. The chlorophylls. *Academic press* INC. 111 fifth Avenue, New York 10003, 1-671.

Wan, J., R. Wang, H. Bai, Y. Wang and J. Xu. 2020. Comparative physiological and metabolomics analysis reveals that single-walled carbon nanohorns and ZnO nanoparticles affect salt tolerance in *Sophora alopecuroides*. *Environ. Sci. Nano*, 7(10): 2968-2981.

Yaashikaa, P.R., P.S. Kumar, S. Jeevanantham and R. Saravanan. 2022. A review on bioremediation approach for heavy metal detoxification and accumulation in plants. *Environ. Pollut.*, 301: 119035.

Zhu, Z., G. Wei, J. Li, Q. Qian and J. Yu. 2004. Silicon alleviates salt stress and increases antioxidant enzymes activity in leaves of salt-stressed cucumber (*Cucumis sativus* L.). *Plant Sci.*, 167(3): 527-533.

Zulfiqar, F. and M. Ashraf. 2021. Nanoparticles potentially mediate salt stress tolerance in plants. *Plant Physiol. Biochem.,* 160: 257-268. DOI: 10.1016/j.plaphy.2021.01.028.